Received: 4 March 2020 | Revised: 11 May 2020 | Accepted: 6 August 2020

DOI: 10.1002/pc.25786

RESEARCH ARTICLE

Polymer COMPOSITES WILEY

Fire behavior of flame retarded sandwich structures containing PET foam cores and epoxy face sheets

Christian Bethke[1] | **Lais Weber**[2,3] | **Daniela Goedderz**[2,3] | **Tobias Standau**[1] | **Manfred Döring**[2] | **Volker Altstädt**[1]

[1]Department of Polymer Engineering, University of Bayreuth, Bayreuth, Germany

[2]Fraunhofer Institute for Structural Durability and System Reliability LBF, Darmstadt, Germany

[3]Ernst-Berl Institute for Chemical Engineering and Macromolecular Science, Technische Universität Darmstadt, Darmstadt, Germany

Correspondence
Volker Altstädt, Department of Polymer Engineering, University of Bayreuth, Universitätsstraße 30, 95447 Bayreuth, Germany.
Email: altstaedt@uni-bayreuth.de

Funding information
German Research Foundation, Grant/Award Numbers: DO 453/9-1, AL 474/28-1

Abstract

Within this work, the investigation on interactions of a phosphorus-containing flame retardant (FR) DEPAl in epoxy face sheets and five different FRs in the PET-foam core of a sandwich laminate on the fire behavior is focused. Fourteen different combinations of resin face sheets and PET foam cores are produced by vacuum assisted resin infusion (VARI). The combustion behavior of the sandwich laminates is tested by cone calorimetry. The time to ignition is lowered when a FR resin is used while the subsequent burning behavior is mainly influenced by the PET foam core. In order to evaluate the interactions of the flame retardants in the core and face sheet, a total improvement value (TIV) was set up which compares the performance related to the specific FR combinations. The highest TIV value (76%) indicating positive interactions with DEPAl was observed with a 2-PSMP-PET core, the lowest value (−2%) with a DEPZn-PET core.

KEYWORDS

flame retardant, sandwich materials, cone calorimetry, PET-foam, composites

1 | INTRODUCTION

Sandwich composite structures offer an excellent balance between lightweight and favorable mechanical properties. They exhibit an advanced performance with regard to specific strength and stiffness, thermal insulation, fatigue endurance, thermal expansion and corrosion resistance compared to comparable bulk and metal alloys. This makes them suitable for applications in transportation and construction sector with increasing demand.[1,2] The foam core provides weight reduction and shear rigidity, whereas the solid skin exhibit significant tensile load bearing and in-plane compressive properties. Next to natural light weight structures such as balsa wood,[3] artificial honey comb structures made of metal or polymers[4] and polymeric foams are applied.[5] Thereof, polymeric foams are most suitable in modern engineering as their properties can be adjusted in a broad range, depending on its basic polymer, its foam morphology and density. Examples for structural foam core materials are polyetherimide (PEI), polyurethane (PU) and polyethylene terephthalate (PET).[3,4,6] Foams with densities as low as 50 kg m^{-3} can be achieved with polymethacrylimide (PMI) or crosslinked polyvinyl chloride (PVC). Recent research also reveals the use of polymer bead foams, for example E-PP or E-PET, as core materials, which allow additionally freedom in shaping and densities down to 15 kg m^{-3}. Among the polymer foams, PET foam cores

provide beneficial aspects such as good solvent resistance, low water uptake, high elastic moduli and impact resistance, as well as good thermal properties.[7] As face sheet materials, typically metals or thermoset resin systems such as acrylic-, epoxy- or phenolic resins are applied. In some cases, also thermoplastic resins such as polypropylene (PP), PET, polyamide (PA) or polyether ether ketone (PEEK) are used.[1,5,8] All thermoplastic composite materials are also applied in some cases, where adapted processing steps are required.[9] However, thermoset face sheets offer benefits with regards to special processing steps for enhanced mechanical properties. Therefore, holes in the core structures allow the resin flow to connect between top and bottom face sheet during infusion setup in order to enhance the interfacial fracture properties.[10] The use of reinforcement fibers, typically glass- or carbon fabrics, additionally increase the mechanical performance of the structural parts.

The application of polymers in the core and face sheet is leading to good adhesion properties between all components, which result in improved mechanical properties and fatigue behavior compared to metal-polymer hybrid systems. However, a high polymer content lowers the fire performance of the structural part compared to metal alloys. High standards in flame retardancy have to be fulfilled especially in the transportation and construction sector. Thus, flame retardants (FRs) are required for most materials to be applicable to those applications. The FR system has to be tailored for each polymer system in order to obtain the best performance.

FR based on halogenated molecules, different phosphorous species, sulfur- and silicon containing additives, melamine species and other inorganic components are used for PET and PBT.[11] Halogenated FRs were likely used in the past due to their high melting points and non-reactivity towards PET.[12] However, environmental and health concerns regarding halogenated FR itself, and the meanwhile known high toxicity of by-products during combustion leads to more and more regulations in the future.[13,14] The broad diversity of inorganic and phosphorus based (P-based) FR is seen as most promising in the future of FR additives.[15,16] The drawback of inorganic fillers is the high amount required for flame-retardant efficiency which can affect the typical material characteristics. Due to its chemical versatility, different P-based flame retardants can be used as reactive component or additive, acting in the gas and/or condensed phase. When mixed in synergistic combinations, the flame-retardant efficiency can be improved even further and thereby with less total amount of flame retardants.[13,17,18]

Common phosphorous species used for FR purpose are phosphinates, phosphonates and phosphates, as well as molecules combining multiple and/or different phosphorus species with various chemical environments of the phosphorous atom.[11,19–23] Köppl et al. investigated the structure—property relationship of P-based FRs, a phosphinate and a phosphinate-phosphonate mixture, in standard and glass fiber reinforced polyesters with concentrations between 4.4 and 20 wt%. A significant influence on mechanical properties and processability, depending on the shape and concentration of the solid FR fillers, was observed. The young's modulus was found to increase with increasing filler contents, however, the elongation at break, tensile- and impact strength was decreased notably by increasing the filler content.[24] A further study investigated polymeric flame retardants based on phosphorus containing polyesters. They were added as immiscible blends to the PBT matrix. Depending on the polymer backbone of the polymeric FR, compatibilization effects with the matrix could be monitored. The fire behavior remained adequate with all types of polymeric FRs. However, the influence on the mechanical properties was found to be strongly dependent on the blend compatibilization. The PBT-co-PET-O-DOPO flame retardant showed less influence on mechanical properties compared to the PET-P-DOPO, showing the highest deterioration of the mechanical properties.[25] Carosio et al. evaluated poly ammonium phosphates for layer by layer coating techniques on PET foams, which allow to generate a protective layer on fine surface structures such as foam cells, without the need for further FR additives in the core.[26] There are also techniques described where the matrix material of core and face sheet is made of all the same material but with a gradual porosity of the laminate setup. In this case, the functional additives, for example, FRs, are located in high concentration at the outer layers with decreasing amount to the center region of the laminate setup, going along with an increase of porosity from outer to core region. This gradual setup reduces the influence of FRs on the foaming, as the foamed core contains less FRs than the compact skin layers. Thus, FRs can be used which interact negatively on foaming for the compact layers.[27]

Common tests for sandwich materials are proceeded in real case scenarios or downscaled related test setups for sandwich panels, such as ISO 13784 (Reaction to fire tests for sandwich panel building systems).[28–30] For the construction sector, more standards such as DIN EN ISO 1524 or 1716 and DIN EN 13823 or 11 925 are established. Evaluating the fire behavior by cone calorimetry is a versatile lab scale method to determine specific flammability and combustion characteristics which is established in the fire science today.[31] The results gained in these lab scale experiments allow conclusions for first material selections for large scale experiments. A study of Xu et al. investigated the thermal behavior and kinetics

of a carbon/epoxy resin composite made of epoxy resin and PVC foam core by TGA-FTIR. They revealed a high activation energy barrier of the pyrolysis reaction with an easy ongoing reaction after overcome of this barrier. A three-step degradation of firstly epoxy matrix, then foam core and finally carbon fibers was observed. Among the combustion gases, next to H_2O and CO_2, hydrocarbons, HCl, and different aromatic compounds were detected.[32]

Within this work, cone calorimetry is used to investigate the fire behavior of sandwich structures made of modified bottle grade PET foam cores and epoxy resin face sheets. Polyesters are known for their low melt strength and therefore often need to be chemically modified to improve the foamability.[33,34] Bottle grade PET and other low IV grades such as recycled PET are highly available with low pricing compared with high molecular PET grades for foaming. Thus, the bottle grade PET foam cores used in this study were produced by reactive foam extrusion (RFE) in the presence of chain extender and different FRs.[35] The FRs used for the RFE were selected by its different chemical environment of the phosphorous in order to investigate its influence in the RFE and to compare it with an established halogen based FR. As p-based FRs, zinc diethyl phosphinate (DEPZn), Pentaerythritol-spirobis(methylphosphonate) (PSMP) and 6H-dibenz[c,e] [1,2]oxaphosphorin,6-[(1-oxido-2,6,7-trioxa-1-phosphabicyclo[2.2.2]oct-4-yl)methoxy]-, 6-oxide (DOP) were chosen. For comparison, the halogen based 1,2-bis(tetrabromophthalimido ethane) (HFR) was selected. More details about the PET-FRs can be found in Data S1. For the PET foams, PSMP and DOP showed best performance regarding the fire behavior. More information about the processing and the properties of the foam cores were presented in our previous work.[35] A study of Mueller et al. evaluated aluminum diethylphosphinate (DEPAl) as suitable flame retardant for epoxy resin made of diglycidylether-of-bisphenole-A (DGEBA) and isophorone diamine (IPDA) with condensed phase activity.[17] Thus, DEPAl was chosen as FR for the resin system in this study.

The aim of this work is to get detailed information of the interactions on the burning behavior of sandwich structures made of different FR modified bottle grade PET foam cores and FR modified epoxy resin face sheets. The different FRs used in the PET foam cores are expected to show different interactions when combined with the FR in the epoxy face sheet.

2 | EXPERIMENTAL

2.1 | Materials

The foam cores were prepared by reactive foam extrusion with different compositions of chain extender and flame retardants.[35] The FRs used in the PET cores are DEPZn, DOP, PSMP, and HFR. A brief summary of the important foam properties and detailed information about the FRs used in the foam core can be found in Table S1. The chemical structures are presented in Figure 1.

The commercially available and flame-retardant PET foam Kerdyn Green (GURIT, Wattwil, Switzerland), further named KD, was used as benchmark regarding PET foam cores.

A standard diglycidylether-of-bisphenole-A (DGEBA) epoxy resin supported as DER331 (Olin, Clayton, MI)

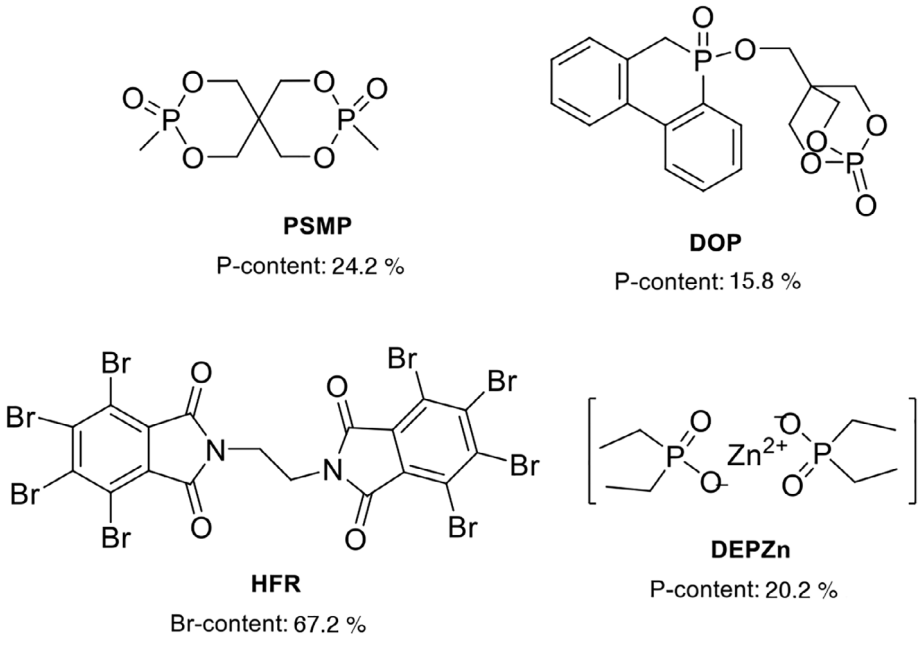

FIGURE 1 Chemical structures of the flame retardants used in the PET cores.[35]

with an epoxy equivalent weight (EEW) of 187 ± 5 g eq^{-1} was used for the infusion process combined with isophorone diamine (IPDA) supported as Aradur 42 BD (Huntsman, Salt Lake City, UT) with an amino hydrogen equivalent weight (AHEW) of 44 ± 2 g eq^{-1} as hardener. The flame retardant for the epoxy matrix is a phosphorus based (aluminum diethylphosphinate, further named DEPAl) flame retardant supported as Exolit OP935 (Clariant, Muttenz, Switzerland) added by 5.22 wt%, corresponding to 1.25% phosphorus content, to the total resin mixture. The chemical structure of the DEPAl FR is shown in Figure 2.

All materials were used as received. As reinforcement of the sandwich structures, one layer of 45° glass fiber fabric (GF, 0.5 mm, 0.7 g cm^{-2}) was set on top and bottom of the PET foam cores. The samples are named by its combination of PET core type and resin type. Table 1 summarizes the combinations of PET-cores and resins of the different investigated sandwich samples.

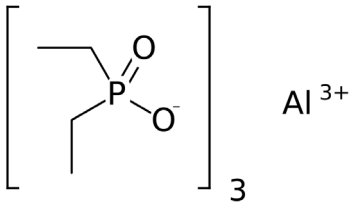

FIGURE 2 Chemical structure of the resin flame-retardant DEPAl

2.2 | Resin sample preparation

The DGEBA and IPDA were used at 100% stoichiometric ratio according to the total amount (m_T) required for each sample. The weight of resin (m_R) was calculated by EEW and AHEW according to Equation (1).

$$m_R(\mathrm{g}) = m_T(\mathrm{g}) \times \left(\frac{\mathrm{EEW}}{(\mathrm{EEW} + \mathrm{AEW})}\right) \quad (1)$$

The weight of hardener (m_H) was calculated by Equation (2):

$$m_H(\mathrm{g}) = m_T - m_R \quad (2)$$

If specified, the resin systems were additionally mixed with DEPAl. The mixtures for the samples containing no GF were poured into an open alumina mold with a gap size of 3 mm for cone calorimetry samples. In order to keep the fiber volume content comparable to the sandwich structures (about one layer GF on 0.6 mm layer resin), six layers of GF fabric were used. The laminates were achieved by RTM processing with an infusion pressure of 2 bar and vacuum. The laminates and mixtures were cured for 120 minutes at 120°C and left at RT in the fume hood afterwards. As release agent, Loctite Frekote 770-NC (Henkel, Düsseldorf, Germany) was used. The final geometries for the Cone Calorimeter (100 mm × 100 mm × 3 mm) were cut with a DiaDisc 2000 saw (Mutronic, Rieden am Forggensee, Germany).

TABLE 1 Sandwich compositions with respective flame retardants used in the foam core and face sheets with the total mass of composite samples

Sample (core + resin)	Mass (g)	Core flame retardant	Resin flame retardant
CE-PET + nR	68.5 ± 2.9	–	–
DEPZn-PET + nR	62.0 ± 1.8	5 wt% DEPZn	–
HFR-PET + nR	85.3 ± 1.2	5 wt% HFR	–
3-PSMP-PET + nR	89.5 ± 4.2	3 wt% PSMP	–
2-PSMP-PET + nR	67.7 ± 1.9	2 wt% PSMP	–
DOP-PET + nR	85.9 ± 1.5	2 wt% DOP	–
KD-PET + nR	51.3 ± 2.7	Unknown	–
CE-PET + FR-R	65.7 ± 0.9	–	5.22 wt% DEPAl
DEPZn-PET + FR-R	58.8 ± 0.6	5 wt% DEPZn	5.22 wt% DEPAl
HFR-PET + FR-R	87.2 ± 0.9	5 wt% HFR	5.22 wt% DEPAl
3-PSMP-PET + FR-R	90.4 ± 9.5	3 wt% PSMP	5.22 wt% DEPAl
2-PSMP-PET + FR-R	62.9 ± 1.8	2 wt% PSMP	5.22 wt% DEPAl
DOP-PET + FR-R	85.9 ± 1.5	2 wt% DOP	5.22 wt% DEPAl
KD-PET + FR-R	48.1 ± 0.2	Unknown	5.22 wt% DEPAl

2.3 | Foam and sandwich sample preparation for cone calorimeter

After the foam extrusion and calibration process, the PET foam sheets show a significant compact skin. In order to obtain homogeneous foam samples, further post processing was required. The preparation steps summarized in Figure 3 are proceeded with all samples to guarantee compatibility.

In order to achieve the sandwich structures, the resin was applied to the foam core by vacuum resin infusion (VARI). A 45° glass fiber fabric (GF) was added on top and bottom of the foam core to complete the sandwich layup. Furthermore, flow aid meshes and a vacuum fleece was applied for proper resin flow.[36] For the infiltration process, a mixture of 100 g DGEBA/IPDA was prepared. Therefore, the DGEBA was pre-heated to 50°C (60°C when containing DEPAl) and mixed with IPDA for 1 minute at 3500 rpm in a DAC 150 speed mixer (Hauschild, Hamm, Germany) at room temperature. Afterwards, the mixture was directly infused into the layup, placed on a heating table at 50°C, at a vacuum of max. 10 mbar. After the infusion process, the setup was sealed and set into a convection oven (Vötsch, Reiskirchen, Germany) at 50°C for 180 minutes. The resulting sandwich materials were post-processed with a band grinder if required in order to remove sharp edges.

2.4 | Flame-retardant testing

The flame-retardant properties were investigated by a cone calorimeter (iCone by *Fire Testing Technology Limited* UK with Servomex Xentra gas analyzer) according to ISO 5660-1-2002. The samples were wrapped into aluminum foil and horizontally set onto the sample holder with a distance of 25 mm to the cone heater. A heat flux of 35 kW m^{-2} was applied for all measurements.

3 | RESULTS AND DISCUSSION

3.1 | Flame-retardant testing

In a first step, the influence of the DEPAl (1.25 wt% phosphorus) on the burning behavior was investigated. Neat resin samples (nR) and samples containing DEPAl (FR-Rare) are investigated, as well as their corresponding GF-containing samples nR-GF and FR-R-GF. The results were evaluated with regards to time to ignition (TTI), peak heat release rate (pHRR), total heat release (THR), the maximum average heat release rate (MARHE) and total smoke release (TSR). The heat release rate over time of the neat resin and the resin containing DEPAl (1.25% P) and their corresponding GF samples are shown in Figure 4 and Table 2.

As observed from Figure 4, the GF samples show different burning behavior compared with the samples without GF. The numerical values of TTI, PHRR, and MARHE as well as the sample weight (m_s) and the wt% GF are summarized in Table 2.

Due to lower content of resin, the samples containing no GF and the samples containing GF have to be compared separately. In order to draw a certain relation, the THR and TSR values were related to the effective combustible mass (m_c). This means, a value for THR and TSR per gram combustible material, and thus without GF which is included with 7 g per layer in the total sample weight (m_s). The calculation of m_c was conducted according to Equation (3):

$$m_c = m_s - m_{GF} \tag{3}$$

In the following, a ratio between m_c and m_s (r_m) can be set up according to Equation (4):

$$r_m = \frac{m_c}{m_s} \tag{4}$$

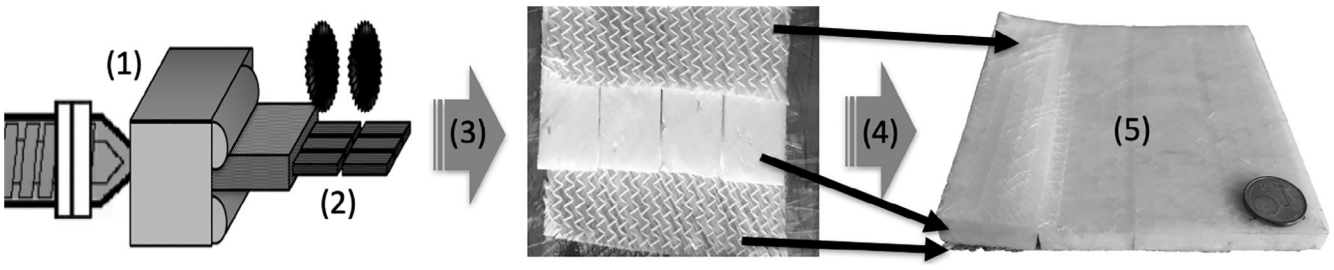

FIGURE 3 Scheme of sample preparation procedure with (1) foam extrusion and calibration, (2) removal of skin and preparation of 100 mm × 25 mm × 10 mm samples from the core region, (3) packing of sandwiches laminates, (4) VARI proceeding, and (5) final 100 mm × 100 mm × 13 mm cone calorimetry sample (the sample presented was prepared with one open side for proper illustration of final layup GF-core-GF)

This ratio r_m is finally used to correct the values of THT and TSR by the amount of combustible material according to Equations (5) and (6):

$$\mathrm{THR(corr.)} = \frac{\mathrm{THR}}{r_m} \tag{5}$$

$$\mathrm{TSR(corr.)} = \frac{\mathrm{TSR}}{r_m} \tag{6}$$

The results of THR(corr.) and TSR(corr.), summarized in Table 3, allow a better comparison of the burning behavior when comparing the GF samples among each other, as they consider a fully combustible sample. Due to the influences of the GF on the burning behavior, a direct comparison to the samples without GF is not applicable. It has to be noted that for samples without GF r_m is 1 as the entire sample can be seen as combustible.

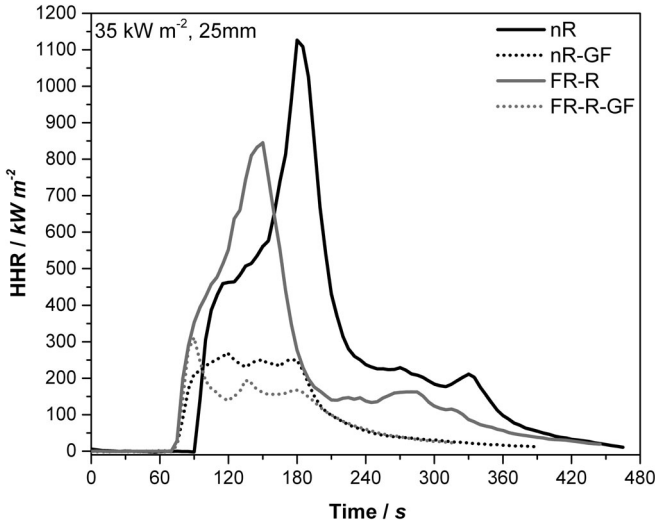

FIGURE 4 HRR curves of the neat resin (nR) and flame retarded with DEPAl (1.25% P) (FR-R) as well as their corresponding glass fiber containing samples nR-GF and FR-R-GF

The addition of DEPAl to the resin containing no GF leads to a reduced TTI by 16 seconds. The PHRR is reduced for FR-R by 28% and the THR by 25%. The TSR could be reduced from 3899 to 3195 $m^2\ m^{-2}$ for FR-R. The GF-containing samples comprise 75 wt% glass fiber start to ignite after 67 seconds (FR-R-GF) and 74 seconds (nR-GF). The PHRR increases by 33% by adding DEPAl, but FR-F-GF shows an initial increase in HRR at the beginning of the burning period which is a result of the formation of a char layer because the following HRR decreases after the char layer is formed. The flame-retardant effect becomes obvious by considering the THR and the MARHE which are both decreased for FR-R-GF by 17%. Taking the THR(corr.) and TSR(corr.) into account for the GF samples, the trend remains the same. However, the decrease in THR(corr.) is more significant, as well as the increase in TSR(corr.) when DEPAl is added.

Figure 5 compares the two resin systems nR and FR-R directly, whereas the neat resin values are set as 100%.

It was observed that the values of pHRR, THR, and TSR can be lowered when DEPAl is added to the system. The results show a decrease in PHRR by 28%, of THR by 25% and of TSR by 18%. The MARHE was decreased from 348 to 29 kW m^{-2}, confirming a proper effectiveness of DEPAl in the resin. When GF are added, the behavior

TABLE 2 Sample weight, wt% GF, time to ignition (TTI), peak heat release rate (PHRR) and maximum average heat release (MARHE) of the resin samples containing FR and or GF and without

Sample (core + resin)	Weight (Sg)	wt% GF	TTI (s)	PHRR (kW m^{-2})	MARHE (kW m^{-2})
nR	43 ± 1	0	93 ± 2	1126 ± 36	348 ± 14
nR-GF	56 ± 1	75	74 ± 13	228 ± 52	139 ± 2
FR-R	39 ± 1	0	77 ± 3	811 ± 31	291 ± 14
FR-R-GF	56 ± 1	75	67 ± 9	303 ± 11	116 ± 7

TABLE 3 Total heat release (THR), THR(corr.), total smoke release TSR and TSR(corr.) as well as the r_m values, of the resin samples containing FR and or GF and without

Sample (resin)	THR (MJ m^{-2})	THR(corr.) (MJ m^{-2})	TSR ($m^2\ m^{-2}$)	TSR(corr.) ($m^2\ m^{-2}$)	r_m
nR	109 ± 3	109	3899 ± 72	3899	1
nR-GF	36 ± 1	145	1068 ± 50	4348	0.25
FR-R	82 ± 2	82	3195 ± 145	3195	1
FR-R-GF	30 ± 2	119	1180 ± 110	4713	0.25

changes. The pHRR is increased slightly compared to nR. As a consequence, the cracking of the initial charring layer, which is supported by the GF, can be seen.

3.2 | Sandwich characteristics

Two different types of epoxy-PET sandwiches were prepared. For each PET-core type, samples with non-flame retarded (nR) and flame retarded (FR-R) glass fiber reinforced epoxy face sheets were prepared. The resulting weight contents of core (core wt%), resin (resin wt%) and GF (GF wt%) of the total sandwich mass are listed in Table 4 and considered in the evaluation of the burning behavior. It also indicates the effective resin uptake of the cores, as the uptake of the fiber fabric can be assumed as constant. As the mass of each sandwich sample ($m_{sandwich}$), core (m_{core}), and GF inlay (m_{GF}) are known, the average resin wt% can be determined as shown in Equation (7):

$$\text{resin wt.}\% = \frac{m_{sandwich} - m_{core} - m_{GF}}{m_{sandwich}} \quad (7)$$

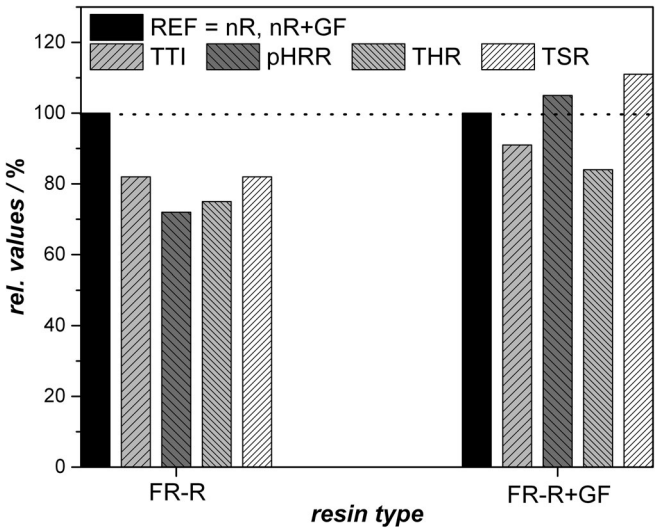

FIGURE 5 Comparison of relative TTI, pHRR, THR, and TSR between neat resin (nR) or NR + GF (=100% for all corresponding values) and resin containing DEPAl as flame retardant (FR-R) or FR-R + GF at 25 mm gap and 35 kw m^{-2} heat flux

The three resulting values for each sample type are averaged and given with SD in Table 4. The total weight of GF for each sandwich structure remains 14 g. However, due to different effects such as core density, core defects and final resin uptake of the sandwich, its effective wt% changes.

The main reason for the deviations in the sample mass is the difference in PET core density and cell size as shown in Table 5.

A certain inhomogeneity of the cell morphology and cell rupture is related to the calibration process, leading to additional voids which might increase the resin uptake. The increased viscosity of FR-R reduces the resin flow into the foam structures, leading to more homogeneous samples as observed by lower standard deviations in the total mass. The homogeneous foam structure of the KD-PET is leading to the highest core wt% values

TABLE 4 Sandwich compositions with respective total average mass and weight of components and its wt% content of core, resin, and GF

		Core		Resin		GF	
Sample (core + resin)	**Mass (g)**	**(g)**	**(wt%)**	**(g)**	**(wt%)**	**(g)**	**(wt%)**
CE-PET + nR	68.5 ± 2.9	15.7	23 ± 1	38.8	57 ± 2	14	20 ± 1
DEPZn-PET + nR	62.0 ± 1.8	20.9	34 ± 1	27.1	44 ± 2	14	23 ± 1
HFR-PET + nR	85.3 ± 1.2	27.6	32 ± 1	43.8	51 ± 1	14	16 ± 1
3-PSMP-PET + nR	89.5 ± 4.2	38.6	43 ± 2	36.9	41 ± 3	14	16 ± 1
2-PSMP-PET + nR	67.7 ± 1.9	23.4	35 ± 1	30.3	45 ± 2	14	20 ± 1
DOP-PET + nR	85.9 ± 1.5	26.8	31 ± 1	45.1	53 ± 1	14	16 ± 1
KD-PET + nR	51.3 ± 2.7	19.0	37 ± 2	18.3	36 ± 3	14	27 ± 2
CE-PET + FR-R	65.7 ± 0.9	15.7	24 ± 1	36.0	55 ± 1	14	21 ± 1
DEPZn-PET + FR-R	58.8 ± 0.6	20.9	36 ± 1	23.8	40 ± 1	14	24 ± 1
HFR-PET + FR-R	87.2 ± 0.9	27.6	32 ± 1	45.7	52 ± 1	14	16 ± 1
3-PSMP-PET + FR-R	93.7 ± 3.8	38.6	43 ± 5	37.8	41 ± 7	14	16 ± 2
2-PSMP-PET + FR-R	62.9 ± 1.8	23.4	34 ± 1	25.5	46 ± 1	14	20 ± 1
DOP-PET + FR-R	85.9 ± 1.5	26.8	31 ± 1	45.1	53 ± 1	14	16 ± 1
KD-PET + FR-R	48.1 ± 0.2	19.0	40 ± 1	15.1	31 ± 1	14	29 ± 1

TABLE 5 Overview of the PET core properties regarding the density of the calibrated foams, cell size and cell density prior to the foam calibration process

PET core	Density cal. (g L^{-1})	Average cell size (μm)	Cell density (cells mm^{-3})
CE-PET	157 ± 8	185 ± 62	4.44×10^5
DEPZn-PET	193 ± 8	193 ± 65	3.79×10^5
HFR-PET	253 ± 24	84 ± 32	6.30×10^6
3-PSMP-PET	401 ± 78	153 ± 66	8.97×10^5
2-PSMP-PET[a]	221 ± 16	94 ± 40	2.36×10^6
DOP-PET	245 ± 16	94 ± 40	4.21×10^6
KD-PET[b]	190 ± 15	292 ± 176	8.27×10^4

[a]Contains ZnSt in a 20:1 ratio PSMP:ZnSt.
[b]Calibrated, evaluated in homogeneous region.

TABLE 6 Cone calorimetry results (irradiation 35 kW m^{-2}) of the epoxy-GF-PET sandwiches (100 mm × 100 mm × 13 mm) with non-flame retarded resin (nR) face sheets. The PHRR reduction is based on the CE-PET + nR value

Sample (core + resin)	TTI (s)	PHRR (kW m^{-2})	PHRR reduction (%)	MARHE (kW m^{-2})
CE-PET + nR	50	598	–	332
DEPZn-PET + nR	40	447	34	206
HFR-PET + nR	55	531	13	290
3-PSMP-PET + nR	64	495	21	258
2-PSMP-PET + nR	55	529	13	218
DOP-PET + nR	53	399	50	224
KD-PET + nR	41	829	−28	259

among all samples, while CE-PET, DOP-PET and HFR-PET samples show high resin wt% as they reveal an overall homogeneous foam structure and the highest cell density (Table 5). This can be explained by a larger surface area due to high amounts of cut open small cells, where the resin can penetrate into the outer layers of the cores, as well as by defects in the foam structures caused by the calibration step. According to these results, a high contribution of the resin to the combustion behavior is expected. The weight content of the GF is varying between 15 and 29 wt% (related to fixed 14 g weight of GF) among the different samples. As the GF can be as assumed to be inflammable, its influence has to be taken into account too.

3.3 | Fire behavior of epoxy-GF-PET sandwiches

Cone calorimetry tests were performed for the different epoxy-GF-PET sandwiches. The results from the tests with neat resin (nR) face sheets and the different PET cores are summarized in Table 6, the values for THR and TSR can be found in Table 8.

As presented in Table 6, notable differences in the burning behavior according to the type of foam core can be observed. An influence of the different FRs on the PET foam cores can be confirmed by the pHRR reduction of all samples when compared to the CE-PET + nR sample. A reduction of the pHRR of the sandwich system up to 50% when containing DOP-PET core can be observed. The benchmark KD-PET foam core however increases the pHRR by 28% when added to the sandwich system. Thus, they are also influenced by the different core densities and weight ratios of core, resin and GF (see Table 4). The fluctuating GF-wt% was considered by using the factor r_m as stated previously. The factor r_m adjusts the TSR and THR values by considering the lower amount of combustible material in the sample due to the glass fibers. It also enables the comparison of samples containing fluctuating process-related amount of glass fibers.[35] The results of the tests with FR-R in the face sheet are summarized in Table 7, the values for THR and TSR are presented in Table 8.

In addition, the THR(corr.) and TSR(corr.) according to Equations (5) and (6) was calculated for the sandwich samples.

The representative HRR curves of the nR and FR-R samples are compared in Figure 6.

As presented in Table 7, as well as observed from Figure 6, the addition of DEPAl to the resin is leading to a lower pHRR among all samples, as well as an increased burning period. A striking effect among all samples, with nR and FR-R, is a second peak in the HRR development due to a cracking of the char which is leading to further pyrolysis in the foam layer of the sample. This effect is less pronounced for the flame retarded face sheet samples because DEPAl promotes the formation of a more dense char layer than the non-flame retarded face sheet. The burning period is elongated for the flame retarded face sheet samples because the formed char layer can prevent the spread of the pyrolysis zone into the foam core for longer time than the non-flame retarded face sheet samples. This effect can be explained by the way of combustion of the sandwich setup, as illustrated in Figure 7.

The first peak in HRR is resulting from the combustion of the top layer glass fiber reinforced epoxy face sheet (1) forming a char layer. While the flame is spreading through the sample, it passes the remaining GF layer, which protects the material below from further heat irradiation of the cone heater in combination with a limited oxygen flow (2). Because of the measurement setup, it is not possible for the sample to get in contact with the air and the flame from the side, as only the top side is accessible (Figure 7). This is resulting in the observed decrease of the HRR. When the flame expanded through the foam core, it reaches the bottom epoxy layer, leading to a second intense combustion process in combination with a formed char layer (3). The second peak remains smaller compared to the first one, as the mentioned effects of shielding from the top GF layer take place in combination with some FR remaining from the PET-cores. The relative performance of the different nR-Sandwiches (=100% reference) to its corresponding FR-R-Sandwich samples is compared in Figure 8A. The effective influence of the combined flame-retardant behavior of core and face-sheet, which is determin0ed by the influence of DEPAl on the resin (Figure 5) and the influence on the burning behavior of the DEPAl on the sandwich structures (Figure 8A), is shown in Figure 8B.

As observed from Figure 8A, the overall burning performance is improved when the resin system is flame retarded, as the resin contributes to more than 30 wt% of combustible material. Because the overall sample weight and the wt% ratio between core, resin and GF are almost similar (Table 4) among the compared PET-core samples, the observed effects can be fully contributed to the interactions of the flame retardants. The TTI is decreasing among all samples when DEPAl is mixed with the epoxy resin, except the sample with DEPZn-PET as core material. The general trend can be contributed to the FR in the resin, as this is also observed for the neat resin plates.

However, the interactions between the different FRs in core and face sheet cannot be observed straightforward. Therefore, the relative performances of the resin itself and the resulting sandwiches with different core materials are compared. Due to the nature of the testing matrix, the influence of DEPAl on the resin system (Figure 5) and the corresponding sandwich laminates (Figure 8A) is known. As the arrangement of the epoxy face sheet of the sandwich laminates is comparable to the resin + GF samples with regards to the FR and GF ratio, a comparable effect of the DEPAl on its burning behavior can be expected. This allows the comparison and understanding of relative trends and values in order to determine the influence of the PET-cores on the overall burning behavior of the sandwich laminates (Figures 5 and 8A).

For example, the TTI is decreasing by 9% when comparing nR + GF with FR-R + GF when DEPAl is added. Comparing CE-PET + nR with CE-PET + FR-R, a decrease of 14% can be observed as a result of the DEPAl

TABLE 7 Cone calorimetry results (irradiation 35 kW m^{-2}) of the modified epoxy-GF-PET sandwiches (100 mm × 100 mm × 13 mm) with FR-R in the face sheets. The PHRR reduction is based on the CE-PET + FR-R value

Sample (core + resin)	TTI (s)	PHRR (kW m^{-2})	PHRR reduction (%)	MARHE (kW m^{-2})
CE-PET + FR-R	43	403	–	174
DEPZn-PET + FR-R	44	399	1	187
HFR-PET + FR-R	48	310	30	156
3-PSMP-PET + FR-R	61	293	38	134
2-PSMP-PET + FR-R	42	388	4	148
DOP-PET + FR-R	51	329	23	141
KD-PET + FR-R	37	482	−17	166

TABLE 8 Total heat release (THR), THR(corr.), total smoke release TSR and TSR(corr.) as well as the r_m values, of the sandwich samples containing FR and without

Sample (core + resin)	THR (MJ m^{-2})	THR(corr.) (MJ m^{-2})	TSR (m^2 m^{-2})	TSR(corr.) (m^2 m^{-2})	r_m
CE-PET + nR	105	132	3419	4298	0.80
DEPZn-PET + nR	74	96	2922	3775	0.77
HFR-PET + nR	114	137	4038	4831	0.84
3-PSMP-PET + nR	118	140	3185	3776	0.84
2-PSMP-PET + nR	88	111	2640	3328	0.79
DOP-PET + nR	96	114	2580	3082	0.84
KD-PET + nR	66	91	2032	2794	0.73
CE-PET + FR-R	80	102	3452	4388	0.79
DEPZn-PET + FR-R	64	84	2668	3501	0.76
HFR-PET + FR-R	91	108	3907	4655	0.84
3-PSMP-PET + FR-R	97	114	2774	3282	0.85
2-PSMP-PET + FR-R	75	94	2148	2692	0.80
DOP-PET + FR-R	86	102	2426	2898	0.84
KD-PET + FR-R	51	71	1797	2534	0.71

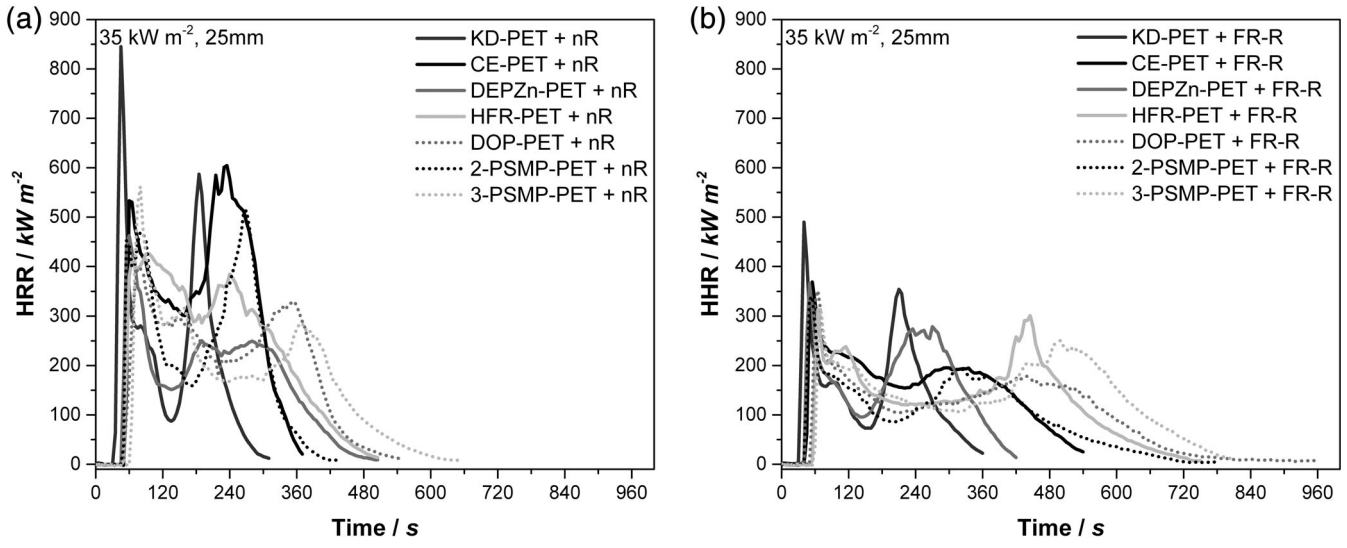

FIGURE 6 Representative HRR curves of (a) sandwich materials without FR in resin and (b) sandwich materials with DEPAl as flame retardant in the face sheet

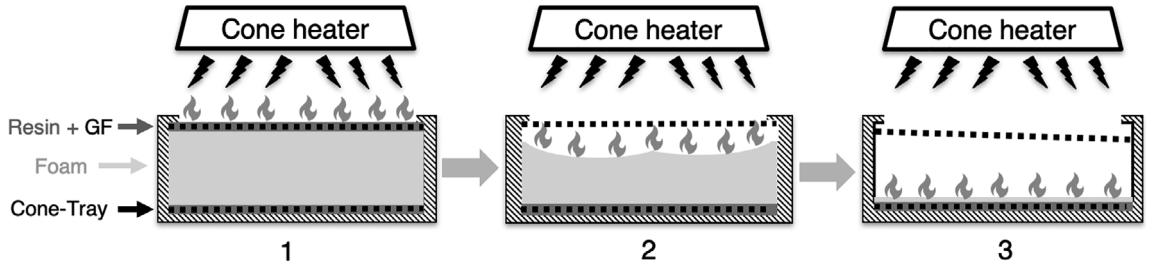

FIGURE 7 Way of combustion of the sandwich structure. (1) ignition and burning of top resin-GF layer, (2) ignition and burning through foam core, and (3) ignition and burning of bottom resin-GF layer

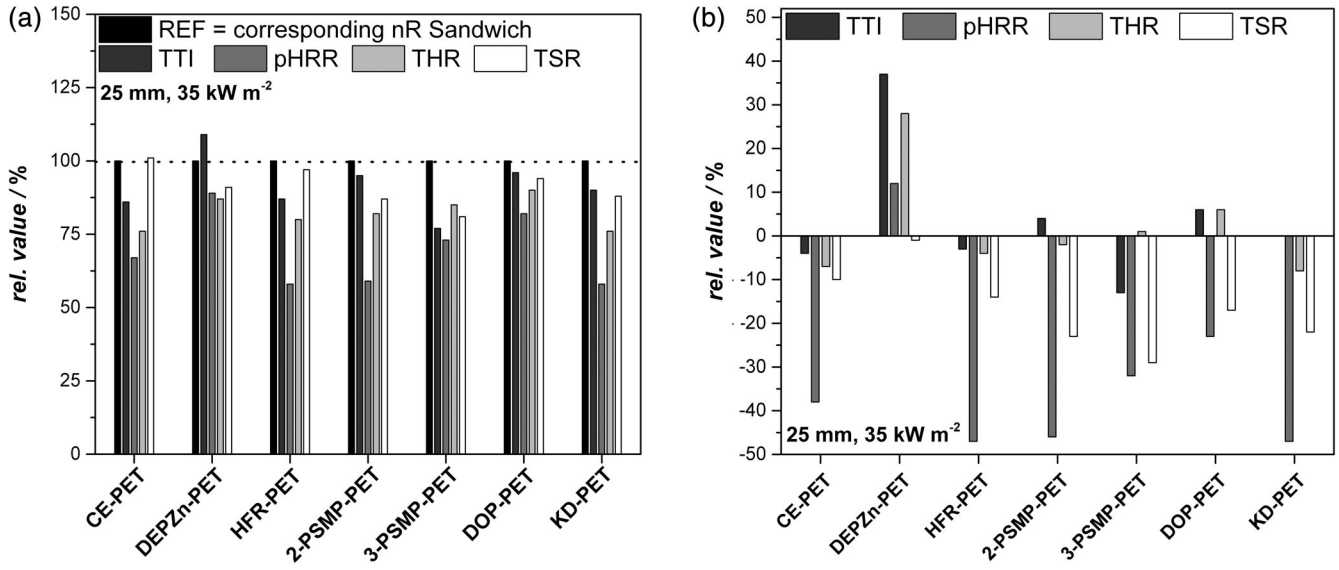

FIGURE 8 (a) Comparison of relative TTI, pHRR, THR, and TSR between sandwiches with nR (=100% for all values) and sandwiches with FR-R and (b) The effective influence of the combined flame-retardant behavior of core and FR-R face-sheet at 25 mm gap and 35 kW m^{-2} heat flux

in the face-sheet. Thus, the overall performance with regard to the TTI is decreased by 4% due to interactions of the PET core with the DEPAl in the face-sheet. This comparison was proceeded for TTI, pHRR, THR, and TSR for every related pair of samples. The results are shown in Figure 8B. In total, all samples show an improvement that can be contributed to the interaction between the individual FR in core and face sheet. The non-flame-retardant core CE-PET show an improvement with regards to pHRR, THR, and TSR. This can be contributed to positive interactions of the PET with the FR in the face sheet, affecting especially the initial burning phase resulting in a lowered pHRR.

In case of DEPZn-PET, the TTI is significantly improved as an interaction of DEPAl and DEPZn, while the pHRR and THR indicate negative interactions with the face sheet by increased values. When 3-PSMP-PET, DOP-PET, and KD-PET are used as core material, the TTI decrease remains as the only draw-back. An effective improvement of all values can be observed for the 2-PSMP-PET core where no notable change in TTI is observed. For better illustration, the relative performances of TTI, pHRR, THR, and TSR can be summed up to get a total % value of improvement (TIV) according to Equation (8):

$$((\mathrm{pHRR} + \mathrm{THR} + \mathrm{TSR}) \times -1) + \mathrm{TTI} = \mathrm{TIV}\,(\%) \qquad (8)$$

The sum of pHRR, THR and TSR is multiplied by −1 as an improvement of these values is resulting in negative values, while a desired elongated TTI is resulting in positive values (Figure 8B). The calculation was proceeded for THR, TSR (TIV) and THR(corr.), TSR(corr.) (TIV-wt) values. The results of TIV and TIV-wt of the sandwich samples are summarized in Figure 9.

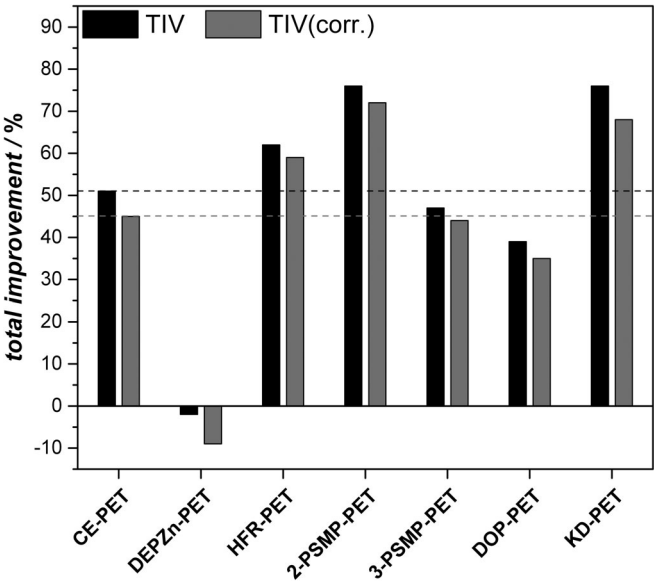

FIGURE 9 Comparison of TIV (black) and TIV(corr.) (grey) values of all samples, whereas positive interactions of the FRs are achieved when the values exceed the value of CE-PET (black or grey line)

The TIV values allow it to compare the overall improvement in the burning behavior at first sight. It can be seen that the weight related TIV(corr.) is resulting in

slightly lower values, as THR(corr.) and TSR(corr.) values are higher. The TIV reveals a value of 51% of CE-PET + FR-R. As samples with DEPZn even reveal a negative value of −2%, the assumption of negative interactions due to the condensed phase activity are confirmed. Samples with DOP-PET (39%) and 3-PSMP-PET (47%) cores reveal lower values compared to a CE-PET core, indicating weak interactions of the FRs. HFR-PET (62%), 2-PSMP-PET (76%) and KD-PET (76%) cores reveal higher TIV values than CE-PET core (51%). Thus, overall improvements in the fire behavior between the foam core and face sheet are proven.

In general, next to the commercial foam core material KD-PET, both core materials HFR-PET and 2-PSMP-PET cores show highest potential when combined with DEPAl in a resin for an improved burning behavior of the sandwich structure, because both have gas phase activity.[37]

4 | CONCLUSION

In conclusion, it is shown that the burning behavior of the foam core in a sandwich composite is affected by interactions with the resin layer from the face sheet and its flame retardant. The observed TTI reduction can be contributed to the FR in the resin face sheet. The pHRR, THR, and TSR could be significantly reduced by the FR in both sandwich systems. As THR and TSR are influenced by the weight of combustible material, THR(corr.) and TSR(corr.) were calculated to provide values for theoretical samples without GF. A total improvement value (TIV) for the sandwich samples containing FR in resin and face sheet was calculated to combine the results for each sample in one value. Here, the total interactions between DEPZn-PET and DEPAl in the resin was found to be less suitable with a TIV of −2%. The non-flame retarded CE-PET (TIV of 51%) revealed also a sufficient performance due to interactions with the DEPAl in the face sheet. DOP-PET (TIV of 39%), 3-PSMP-PET (TIV of 47%) show lower TIV values indicating weak interactions. However, it has been shown that flame retardants with mixed activity in gas- and condensed phase are also suitable for an improved burning behavior of the sandwich composite. The most promising interactions with DEPAl were found with 2-PSMP-PET (TIV of 76%) and HFR-PET (TIV of 62%). This leads to the conclusion that the foam core with mainly gas phase active FRs (PSMP, HFR) has an improved burning behavior in sandwich applications due to the high surface/volume ratio.

ACKNOWLEDGEMENTS

The authors would like to thank the German Research Foundation (DFG) for financial support (project number 278300368: AL 474/28-1 and DO 453/9-1). Furthermore, we would like to thank Prof. Dr. Josef Breu and Florian Puchtler of the Department of Inorganic Chemistry II at the University of Bayreuth for the ability and assistance to proceed the cone measurements, and the Bavarian Polymer Institute (BPI) for the ability to work in their labs and equipment.

NOMENCLATURE

CE-PET	PET foam core made by reactive foam extrusion of bottle grade PET with chain extender, without flame retardant
CE-PET + FR-R	sandwich laminate made of CE-PET core and 5.22 wt% DEPAl resin face sheet, containing two layers of glass fibers
CE-PET + nR	sandwich laminate made of CE-PET core and neat resin face sheet, containing two layers of glass fibers
DEPAl	aluminum diethyl phosphinate
DEPZn	zinc diethyl phosphinate
DOP	6H-dibenz[c,e] [1,2]oxaphosphorin,6-[(1-oxido-2,6,7-trioxa-1-phosphabicyclo[2.2.2]oct-4-yl)methoxy]-, 6-oxide
DOP-PET + FR-R	sandwich laminate made of 2 wt% DOP core and neat 5.22 wt% DEPAl face sheet, containing two layers of glass fibers
DOP-PET + nR	sandwich laminate made of 2 wt% DOP core and neat resin face sheet, containing two layers of glass fibers
DEPZn-PET + FR-R	sandwich laminate made of 5 wt% DEPZn core and 5.22 wt% DEPAl resin face sheet, containing two layers of glass fibers
DEPZn-PET + nR	sandwich laminate made of 5 wt% DEPZn core and neat resin face sheet, containing two layers of glass fibers
FR-R	sample of DEPAl containing resin
FR-R + GF	sample of DEPAl containing resin containing 6 layers of glass fibers (GF) for comparable fiber-volume content to the resin face sheet of sandwich laminates
HFR	1,2-bis(tetrabromophthalimido) ethane

HFR-PET + FR-R	sandwich laminate made of 5 wt% HFR core and 5.22 wt% DEPAl resin face sheet, containing two layers of glass fibers
HFR-PET + nR	sandwich laminate made of 5 wt% HFR core and neat resin face sheet, containing two layers of glass fibers
KD	commercial reference foam core Kerdyn
KD-PET + nR	sandwich laminate made of KD core and neat resin face sheet, containing two layers of glass fibers
KD-PET + FR-R	sandwich laminate made of KD core and 5.22 wt% DEPAl resin face sheet, containing two layers of glass fibers
PSMP	pentaerythritol-spirobis (methylphosphonate)
nR	sample of neat resin
nR + GF	sample of neat resin containing 6 layers of glass fibers (GF) for comparable fiber-volume content to the resin face sheet of sandwich laminates
3-PSMP-PET + nR	sandwich laminate made of 3 wt% PSMP core and neat resin face sheet, containing two layers of glass fibers
2-PSMP-PET + nR	sandwich laminate made of 2 wt% PSMP core and neat resin face sheet, containing two layers of glass fibers
3-PSMP-PET + FR-R	sandwich laminate made of 3 wt% PSMP core and 5.22 wt% DEPAl resin face sheet, containing two layers of glass fibers
2-PSMP-PET + FR-R	sandwich laminate made of 2 wt% PSMP core and 5.22 wt% DEPAl resin face sheet, containing two layers of glass fibers

ORCID

Volker Altstädt https://orcid.org/0000-0003-0312-6226

REFERENCES

[1] A. P. Mouritz, A. G. Gibson, *Fire Properties of Polymer Composite Materials*, Springer, Dordrecht, Netherlands **2006**.
[2] J. Schmied, D. C. Ruff, *Stahlbau* **2015**, *11*, 862.
[3] A. Fathi, F. Wolff-Fabris, V. Altstädt, R. Gätzi, *J. Sandwich Struct. Mater.* **2013**, *15*, 487.
[4] M. Akay, R. Hanna, *Composites* **1990**, *21*, 325.
[5] P. Schreier, T. Neumeyer, J. Knöchel, Presented at ICSS-12, Lausanne – Switzerland, August **2018**, https://10.5075/epfl-ICSS12-2018-161-163.
[6] T. Khan, V. Acar, M. R. Aydin, B. Hülagü, H. Akbulut, M. Ö. Seydibeyoglu, *Polym. Compos.* **2020**, *41*, 2335.
[7] L. Sorrentino, E. Di Maio, S. Iannace, *J. Appl. Polym. Sci.* **2010**, *116*, 27.
[8] P. Brøndstedt, H. Lilholt, A. Lystrup, *Annu. Rev. Mater. Res.* **2005**, *35*, 505.
[9] U. Breuer, M. Ostgathe, M. Neitzel, *Polym. Compos.* **1998**, *19*, 275.
[10] H. Z. Jishi, R. Umer, W. J. Cantwell, *Polym. Compos.* **2016**, *37*, 2974.
[11] S. V. Levchik, E. D. Weil, *Poly. Int.* **2005**, *54*, 11.
[12] A. G. Hussain, G. Arianna, S. Tonino (SINCO RICERCHE S.p. A.), EP0908488 A1, **1999**
[13] M. M. Velencoso, A. Battig, J. C. Markwart, B. Schartel, F. R. Wurm, *Angew. Chem., Int. Ed.* **2018**, *57*, 10450.
[14] S. D. Shaw, A. Blum, R. Weber, K. Kannan, D. Rich, D. Lucas, C. P. Koshland, D. Dobraca, S. Hanson, L. S. Birnbaum, *Rev. Environ. Health* **2010**, *25*, 261.
[15] J. Zhang, Q. Ji, P. Zhang, Y. Xia, Q. Kong, *Polym. Deg. Stab.* **2010**, *95*, 1211.
[16] J. Li, H. Grater (Armacell Enterprise GmbH & Co, Kg,), US20100305224 A1, 2010
[17] P. Müller, B. Schartel, *J. Appl. Polym. Sci.* **2016**, *133*, 1.
[18] D. Goedderz, L. Weber, *J. Appl. Polym. Sci.* **2019**, *47876*, 1.
[19] A. Hörold, B. Schartel, V. Trappe, M. Korzen, J. Bünker, *Compos. Struct.* **2016**, *160*, 1.
[20] Y. Fang, X. Zhou, Z. Xing, Y. Wu, *J. Appl. Polym. Sci.* **2017**, *134*, 1.
[21] B. Perret, B. Schartel, K. Stöß, M. Ciesielski, J. Diederichs, M. Döring, J. Krämer, V. Altstädt, *Eur. Polym. J.* **2011**, *47*, 1081.
[22] B. Perret, B. Schartel, K. Stöß, M. Ciesielski, J. Diederichs, M. Döring, J. Krämer, V. Altstädt, *Macromol. Mater. Eng.* **2011**, *296*, 14.
[23] U. Braun, B. Schartel, *Macromol. Mater. Eng.* **2008**, *293*, 206.
[24] T. Köppl, S. Brehme, F. Wolff-Fabris, *J. Appl. Polym. Sci.* **2011**, *124*, 9.
[25] T. Köppl, S. Brehme, D. Pospiech, *J. Appl. Polym. Sci.* **2013**, *128*, 3315.
[26] P. Carosio, F. Cuttica, A. D. Blasio, *Polym. Deg. Stab.* **2015**, *113*, 189.
[27] J. Weidinger, M. Meller, J. Li (Armacell Enterprise GmbH & Co, Kg), US9005701 B2, **2015**
[28] R. R. Leisted, M. X. Sørensen, G. Jomaas, *Fire Saf. J.* **2017**, *93*, 114.
[29] E. Pastor, B. Corberó, O. Rios, M. P. Giraldo, L. Haurie, A. Lacasta, E. Cuerva, E. Planas, presented at Appl. of Struct. fire Engin., Dubrovnik Croatia, 15–16 October **2015**
[30] K.-W. Park, M. Mizuno, K. Ikeda, Y. Ohmiya, S. Sugahara, Y. Hayashi, *J. Asian Arch. Build. Eng.* **2015**, *14*, 695.
[31] B. Schartel, T. T. Hull, *Fire Mater.* **2007**, *31*, 327.
[32] Y. Xu, Y. Yang, R. Shen, T. Parker, Y. Zhang, Z. Wang, Q. Wang, *Polym. Compos.* **2019**, *40*, 4530.
[33] T. Standau, B. Hädelt, P. Schreier, *Ind. Eng. Chem. Res.* **2018**, *57*, 17170.
[34] T. Standau, C. Zhao, S. M. Castellón, *Polymer* **2019**, *11*, 206.
[35] C. Bethke, D. Goedderz, L. Weber, T. Standau, M. Döring, V. Altstädt, *J. Appl. Polym. Sci.* **2020**, *137*, e49042.
[36] H. M. Anderson, T. S. Lundsröm, B. R. Gebhart, R. Langström, *Polym. Compos.* **2002**, *23*, 895.
[37] C. Geschwindner, D. Goedderz, T. Li, C. Fasel, R. Riedel, V. Altstädt, C. Bethke, F. Puchtler, J. Breu, M. Döring, A. Dreizler, B. Böhm, *Exp. Fluids* **2020**, *61*, 1.

SUPPORTING INFORMATION

Additional supporting information may be found online in the Supporting Information section at the end of this article.

How to cite this article: Bethke C, Weber L, Goedderz D, Standau T, Döring M, Altstädt V. Fire behavior of flame retarded sandwich structures containing PET foam cores and epoxy face sheets. *Polymer Composites*. 2020;41:5195–5208. https://doi.org/10.1002/pc.25786